

Reactive oxygen species and nitric oxide regulate mitochondria-dependent apoptosis and autophagy in evodiamine-treated human cervix carcinoma HeLa cells

JIA YANG^{1,2}, LI-JUN WU², SHIN-ICHI TASHINO³, SATOSHI ONODERA³, & TAKASHI IKEJIMA¹

¹China-Japan Research Institute of Medical and Pharmaceutical Sciences, ²Department of Phytochemistry, Shenyang Pharmaceutical University, Shenyang 110016, PR China, and ³Department of Clinical and Biomedical Sciences, Showa Pharmaceutical University, Tokyo 194-8543, Japan

Accepted by Professor N. Taniguchi

(Received 18 February 2008; in revised form 30 March 2008)

Abstract

The redox environment of the cell is currently thought to be extremely important to control either apoptosis or autophagy. This study reported that reactive oxygen species (ROS) and nitric oxide (NO) generations were induced by evodiamine time-dependently; while they acted in synergy to trigger mitochondria-dependent apoptosis by induction of mitochondrial membrane permeabilization (MMP) through increasing the Bax/Bcl-2 or Bcl-x_L ratio. Autophagy was also stimulated by evodiamine, as demonstrated by the positive autophagosome-specific dye monodansylcadaverine (MDC) staining as well as the expressions of autophagy-related proteins, Beclin 1 and LC3. Pre-treatment with 3-MA, the specific inhibitor for autophagy, dose-dependently decreased cell viability, indicating a survival function of autophagy. Importantly, autophagy was found to be promoted or inhibited by ROS/NO in response to the severity of oxidative stress. These findings could help shed light on the complex regulation of intracellular redox status on the balance of autophagy and apoptosis in anti-cancer therapies.

Keywords: *Reactive oxygen species (ROS), nitric oxide (NO), apoptosis, autophagy, evodiamine*

Introduction

Apoptosis, or programmed cell death, is a genetically regulated cell suicide process, which plays an essential role in the development and homeostasis of higher organisms [1]. Disruption of the apoptotic pathway leads to autoimmunity, neurodegenerative disorders, acquired immune deficiency syndrome and all types of cancer [2]. Mitochondria are acknowledged as the central coordinators of apoptotic events to determine the intrinsic pathway of apoptosis. Several intracellular signals converge on mitochondria to induce mitochondrial membrane permeabilization (MMP), which

causes the dissipation of mitochondrial transmembrane potential ($\Delta\Psi_m$) and the release of proapoptotic factors. Release of cytochrome *c*, the apoptogenic factor which is regulated by the anti- and pro-apoptotic members of the Bcl-2 family, from mitochondria, leads to the activation of caspases and subsequent cell death [3]. Thus, many parameters of mitochondrial physiology, including the loss of $\Delta\Psi_m$ and the release of cytochrome *c*, have been shown to be hallmarks of mitochondria-dependent apoptosis [4].

Autophagy sometimes occurs with apoptosis in the process of programmed cell death. It plays a critical

Correspondence: T. Ikejima, China-Japan Research Institute of Medical and Pharmaceutical Sciences, Shenyang Pharmaceutical University, 103 Wenhua Road, Shenyang 110016, Liaoning Province, PR China. Tel/Fax: 86 24 23844463. Email: ikejimat@vip.sina.com

role in removing damaged or surplus organelles in order to maintain cellular homeostasis. There are three main types of autophagy: macroautophagy, microautophagy and chaperone-mediated autophagy [5]. Macroautophagy (hereafter referred to as autophagy) is the most prevalent form of autophagy and is characterized by the formation of a double-membrane bound vacuole called autophagosome. The autophagic process is executed with the sequestration of cytoplasmic material within autophagosomes, which then fuse with lysosomes to create autolysosomes, resulting in the digestion and ultimate recycling of the sequestered contents [6]. Different autophagy proteins (Atg) have specific functions from initiation to elongation to termination of the process. Among which, LC3 (microtubule-associated protein 1 light chain 3), the mammalian homologue of yeast Atg8, is associated with the elongation of the phagophore and the formation of the autophagosome. Beclin1, the mammalian homologue of yeast Atg6, is also a positive regulator of the autophagic vacuole formation [7].

The redox environment of the cell is currently thought to be extremely important to control either apoptosis or autophagy as many redox-sensitive proteins characterize these networks. There are two major forms of free radicals, reactive oxygen species (ROS) and nitric oxide (NO), which are formed from oxygen and nitrogen. Under normal conditions, ROS are cleared by antioxidant enzymes including catalase (CAT), superoxide dismutase (SOD); upon stress stimuli, an imbalance of the redox milieu develops and leads to the accumulation of ROS, which results in oxidative stress [8]. Another gaseous free radical, NO, has been identified as a fundamental molecule that interplays with ROS in a variety of ways, either as a crucial partner in regulating the redox status of the cell, determining cell fate or in signalling in response to a number of physiological and stress-related conditions [9]. The particular outcome varies depending on cell types as well as the redox status.

Evodiamine is a quinoxaline alkaloid isolated from the dried, unripe fruit of *Evodia rutaecarpa* Benth (Rutaceae) and was found to present anti-tumour growth, anti-obesity, anti-anoxic, anti-nociceptive and vasorelaxant effects [10–14]. It has been shown that ROS and NO were both triggered by evodiamine to induce human melanoma A375-S2 cell apoptosis in our previous studies [15,16]. In this study, we provided a detailed look at the effect of evodiamine treatment on human cervix carcinoma HeLa cells. The possible involvements and the related mechanisms of ROS and NO in regulating apoptosis and autophagy following evodiamine administration would be discussed.

Materials and methods

Reagents

Evodiamine was obtained from Beijing Institute of Biological Products (Beijing, China); and its purity was determined to be ~98% by HPLC measurement. Evodiamine was dissolved in dimethyl sulphoxide (DMSO) to make a stock solution and diluted by RPMI-1640 (Gibco, Grand Island, NY) before the experiments. DMSO concentration in all cell cultures was kept below 0.001%, which had no detectable effect on cell growth or death. 3-(4,5-dimethylthiazol-2-yl)-2,5-diphenyltetrazolium bromide (MTT), 3,3-diaminobenzidine tetrahydrochloride (DAB), catalase (CAT), N^G-nitro-L-arginine methyl ester (L-NAME), acridine orange (AO), 2',7'-dichlorofluorescein diacetate (DCF-DA), 4,5-diaminofluorescein diacetate (DAF-2DA), lipopolysaccharide (LPS), rhodamine-123, monodansylcadaverine (MDC), 3-methyladenine (3-MA), PMSF, aprotinin and leupeptin were purchased from Sigma Chemical (St. Louis, MO). Polyclonal antibodies against iNOS, β -actin, caspase-3, ICAD, Bax, Bcl-2, Bcl-x_L, cytochrome *c*, Beclin 1, LC3 and horseradish peroxidase-conjugated secondary antibodies were obtained from Santa Cruz Biotechnology (Santa Cruz, CA).

Cell culture

HeLa, human cervix carcinoma cells, were obtained from American Type Culture Collection (ATCC, #CCL-2, Manassas, VA) and were cultured in RPMI-1640 medium supplemented with 10% heat inactivated (56°C, 30 min) foetal calf serum (Beijing Yuanheng Shengma Research Institution of Biotechnology, Beijing, China), 2 mM L-glutamine (Gibco, Grand Island, NY), 100 kU/L penicillin and 100 g/L streptomycin (Gibco) at 37°C in 5% CO₂. Cells in the exponential phase of growth were used in the experiments.

Assessment of cell viability

HeLa cells were dispensed in 96-well flat bottom microtiter plates (NUNC, Roskilde, Denmark) at a density of 1×10^5 cells/ml. After 12 h incubation, the cells were treated with or without CAT, L-NAME or 3-MA at given concentrations 1 h prior to the administration of evodiamine for the indicated time periods. Cell viability was measured using the MTT assay as described elsewhere [17] with a plate reader (Bio-Rad, Hercules, CA). The percentage of cell viability was calculated as follows:

$$\text{Cell viability (\%)} = \frac{(\text{A490, sample-A490, blank})}{(\text{A490, control-A490, blank})} \times 100$$

LDH activity-based cytotoxicity assay

LDH (lactate dehydrogenase) activity was assessed using a standardized kinetic determination kit (Zhongsheng LDH kit, Beijing, China). LDH activity was measured in both floating dead cells and viable adherent cells [18]. The floating cells were collected from culture medium by centrifugation ($240 \times g$) at 4°C for 5 min and the LDH content from the pellets was used as an index of apoptotic cell death (LDHp). The LDH released in the culture medium (extracellular LDH or LDHe) was used as an index of necrotic death and the LDH present in the adherent viable cells as intracellular LDH (LDHi). The percentage of apoptotic and necrotic cell death was calculated as follows:

$$\text{Apoptosis\%} = \frac{\text{LDHp}}{\text{LDHp} + \text{LDHi} + \text{LDHe}} \times 100$$

$$\text{Necrosis\%} = \frac{\text{LDHe}}{\text{LDHp} + \text{LDHi} + \text{LDHe}} \times 100$$

Observation of morphologic changes

HeLa cells were dispensed in 6-well culture plates at a density of 1×10^5 cells/ml. After 12 h incubation, the cells were treated with or without 4 mM 3-MA 1 h prior to the administration of 21 μM evodiamine for 24 h incubation. The cellular morphology was then observed using phase contrast microscopy (Leica, Wetzlar, Germany).

Nuclear damage observed by acridine orange (AO) staining

The changes in nuclear morphology of apoptotic cells were investigated by labelling cells with the fluorescent, selective DNA and RNA-binding dye AO and examined under fluorescent microscopy (Green fluorescence for DNA, red fluorescence for RNA) [19]. After treatment with or without 21 μM evodiamine for 24 h, the cells were stained with 20 $\mu\text{g/ml}$ AO for 15 min and then the nuclear morphology was observed under fluorescence microscopy (Olympus, Tokyo).

Measurement of intracellular ROS generation

After treatment with 21 μM evodiamine for the indicated time periods in the presence or absence of 1000 U/ml CAT, the cells were incubated with 10 μM 2',7'-dichlorofluorescein diacetate (DCF-DA) at 37°C for 15 min to assess ROS-mediated oxidation of DCF-DA to the fluorescent compound 2',7'-dichlorofluorescein (DCF). Then the cells were harvested and the pellets were suspended in 1 ml PBS. Samples were analysed at an excitation wavelength of 480 nm and an emission wavelength of 525 nm by a FACScan flowcytometry (Becton Dickinson, Franklin Lakes, NJ) [20].

Measurement of intracellular NO generation

The intracellular NO was detected using DAF-2DA as described by Habel and Jung [21] with some modifications. DAF-2DA, a nitric oxide fluorescent probe, can react with NO within viable cells to produce a fluorescent compound DAF-2T. After drug treatment, the cells were collected and resuspended in PBS and then incubated with 10 μM DAF-2DA at 37°C for 45 min. Samples were then analysed at an excitation wavelength of 485 nm and an emission wavelength of 515 nm by FACScan flowcytometry (Becton Dickinson, Franklin Lakes, NJ).

Measurement of $\Delta\Psi\text{m}$

$\Delta\Psi\text{m}$ was measured by the incorporation of a cationic fluorescent dye rhodamine 123 as described [22]. After incubation with 21 μM evodiamine for the indicated time periods, the cells were stained with 1 $\mu\text{g/ml}$ rhodamine 123 and incubated at 37°C for 15 min. The fluorescence intensity of cells *in situ* was observed under fluorescence microscopy. Quantitative assay was performed by a similar staining procedure as above. After treatment with evodiamine, the cells were instead collected and suspended in 1 ml PBS containing 1 $\mu\text{g/ml}$ rhodamine 123 and incubated at 37°C for 15 min. The fluorescence intensity of cells was analysed within 15 min by FACScan flowcytometry (Becton Dickinson, Franklin Lakes, NJ).

Isolation of cytosolic and mitochondrial fractions

The tested cell groups were collected by centrifugation at $200 \times g$ at 4°C for 5 min and then washed twice with ice-cold PBS. The cell pellets were resuspended in ice-cold homogenizing buffer, including 250 mM sucrose, 20 mM HEPES, 10 mM KCl, 1 mM EDTA, 1 mM EGTA, 1.5 mM MgCl_2 , 1 mM DTT, 1 mM PMSF, 1 $\mu\text{g/ml}$ aprotinin and 1 $\mu\text{g/ml}$ leupeptin. After homogenization (40 strokes), the homogenates were centrifuged at $4200 \times g$ at 4°C for 30 min. The supernatant was used as the cytosol fraction and the pellet was resolved in lysis buffer as the mitochondria fraction [23].

Isolation of cytosolic and nuclear fractions

Extracts were prepared essentially according to the method by Zanna et al. [24]. Cells were washed twice with ice-cold Hanks' balanced salt solution before resuspension in 10 mM HEPES pH 7.9, 10 mM KCl, 1.5 mM MgCl_2 , 0.1% v/v Nonidet P40 (Nonidet P-40), 0.5 mM phenylmethylsulphonyl fluoride (PMSF) and 1 mM dithiothreitol (DTT). After incubation on ice for 2 min, nuclei were separated by centrifugation at $1000 \times g$ for 10 min. Supernatants (cytoplasmic extracts) were retained.

Western blot analysis

HeLa cells were treated with 21 μM evodiamine for 0, 6, 12 or 24 h or co-incubated with the given inhibitors for 24 h. Both adherent and floating cells were collected and then Western blot analysis was carried out as previously described [25] with some modification. Briefly, the cell pellets were resuspended in lysis buffer, including 50 mM Hepes (pH 7.4), 1% Triton-X 100, 2 mM sodium orthovanadate, 100 mM sodium fluoride, 1 mM edetic acid, 1 mM PMSF (Sigma), 10 $\mu\text{g}/\text{mL}$ aprotinin, 10 $\mu\text{g}/\text{mL}$ leupeptin and lysed on ice for 60 min. After centrifugation of the cell suspension at 13 000 $\times g$ for 15 min, the protein content of supernatant was determined by Bio-Rad protein assay reagent (Bio-Rad, Hercules, CA). The protein lysates were separated by electrophoresis in 12% SDS-polyacrylamide gel electrophoresis and blotted onto nitrocellulose membrane (Amersham Biosciences, Piscataway, NJ). Proteins were detected using polyclonal antibody and visualized using anti-rabbit, anti-mouse, or anti-goat IgG conjugated with horseradish peroxidase (HRP) and 3,3-diaminobenzidine tetrahydrochloride (DAB) as the substrate of HRP.

Flowcytometric analysis of autophagy

HeLa cells were treated with 1000 U/ml CAT, 20 mM L-NAME or 4 mM 3-MA 1 h before 21 μM evodiamine administration. After the indicated time periods, the cells were harvested by trypsin and rinsed with PBS twice by centrifugation at 1500 $\times g$. For measuring autophagy, the cell pellet was suspended with 0.05 mM MDC solution at 37°C for 60 min as described [26].

Statistical analysis

The results are presented as Mean \pm SD. Comparisons between groups were made using Student's *t*-test. A *p*-value less than 0.05 was considered to represent a statistically significant difference.

Results

The predominant mechanism responsible for evodiamine-induced cell death was apoptosis

As shown in Figure 1A, treatment of HeLa cells with increasing concentrations of evodiamine for 6, 12, 24 and 36 h resulted in a concentration- and time-dependent decrease of cell viability, as measured by MTT assay. Evodiamine from 2.5 to 80 μM exerted a significant induction of cell loss and treatment with 21 μM evodiamine for 24 h resulted in almost 50% inhibition. To examine whether apoptosis was triggered by evodiamine, we observed the morphologic changes in the cells. When the cells were cultured with 21 μM evodiamine for 24 h, small apoptotic

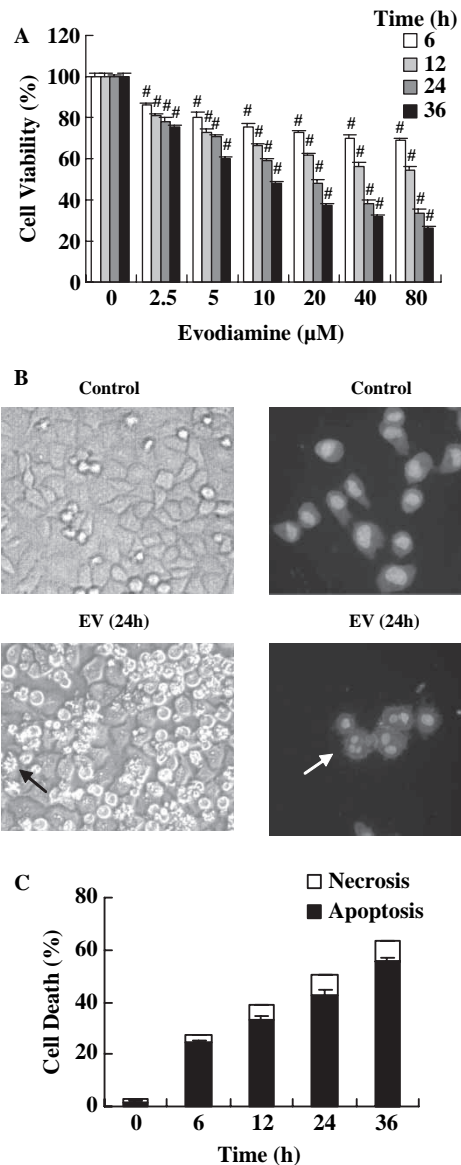


Figure 1. Evodiamine induced apoptosis in HeLa cells. (A) The cells were treated with various doses of evodiamine for 6, 12, 24 or 36 h. The viability of cell was measured by MTT assay ($n=3$, Mean \pm SD, # $p < 0.01$ compared to the control groups). (B) The cellular morphologic changes were observed after cells incubated with medium or 21 μM evodiamine for 24 h under a phase contrast microscope (arrow indicates apoptotic body; $\times 200$ magnification) or under a fluorescence microscope by AO staining (arrow indicates fragmented nuclear DNA; $\times 200$ magnification). (C) The cell death rate was measured by LDH activity-based assay after cells incubated with 21 μM evodiamine for 0, 6, 12, 24 or 36 h. Values are expressed as mean \pm SD.

bodies were observed (Figure 1B). In addition, apoptosis were also observed followed by AO staining. In the control group, the nuclei in which DNA resides were round and homogeneously stained, whereas the evodiamine-treated cells showed marked fragmented nuclei (Figure 1B). These phenomena all suggested that apoptotic cell death was induced by evodiamine in HeLa cells. To further investigate the characteristics of cell death induced by evodiamine,

ratios of apoptosis and necrosis were analysed by LDH activity-based assay. Incubation with 21 μM evodiamine for increasing time periods, the number of apoptotic cells was increased significantly to 24.5% at 6 h, 33.2% at 12 h, 42.9% at 24 h or 55.5% at 36 h, respectively; while the number of necrotic cells remained below 7.7% in 36 h treatment with a slight time-dependent increase (Figure 1C). Therefore, apoptosis was the predominant mechanism responsible for evodiamine-induced cell death.

Evodiamine-induced intracellular ROS generation in HeLa cells

To determine whether ROS was triggered in evodiamine-treated HeLa cells, the intracellular ROS level was measured by flow cytometry after being labelled with DCF-DA, a specific ROS-detecting fluorescent dye. Exposure of HeLa cells to 21 μM evodiamine for 6, 24 or 36 h led to a marked increase in DCF fluorescence compared with the control group. The ratio of DCF positive cells was increased from 2.3% in untreated cells to 16.8%, 67.4% or 74.3% in 6, 24 or 36 h-treated cells, respectively (Figure 2). When pre-treated with the antioxidant enzyme CAT, which could provide a protective role against the destructive effects of ROS, the corresponding burst of DCF fluorescence was largely reduced to 3.0%, 21.8% or

25.2% at 6 h, 24 h or 36 h incubation with evodiamine (Figure 2). Therefore, ROS generation was stimulated by evodiamine in HeLa cells.

Evodiamine induced intracellular NO generation in HeLa cells

To investigate whether NO was produced in evodiamine-treated cells, the intracellular NO level was examined by using DAF-2DA, a membrane-permeable derivative of the NO sensitive fluorophore DAF-2. The reaction of NO with DAF-2 yields the green fluorescent triazole derivative DAF-2T [27]. Exposure of HeLa cells to 21 μM evodiamine for 6, 24 or 36 h led to a remarkable time-dependent enhancement in DAF-2T staining compared with the control group. The ratio of DAF-2T positive cells was increased from 1.9% in untreated cells to 10.4%, 45.3% or 56.3% in 6, 24 or 36 h-treated cells, respectively (Figure 3A). When pre-treated with the inducible NO synthase (iNOS) inhibitor L-NAME, a methyl ester derivative of the NOS substrate L-arginine, the burst of DAF-2T fluorescence was markedly reduced to 2.9%, 17.5% or 19.2% at 6 h, 24 h or 36 h treatment with evodiamine (Figure 3A). Moreover, the expression of iNOS enzyme was detected by Western blot analysis. As shown in Figure 3B, treatment of HeLa cells with evodiamine caused a

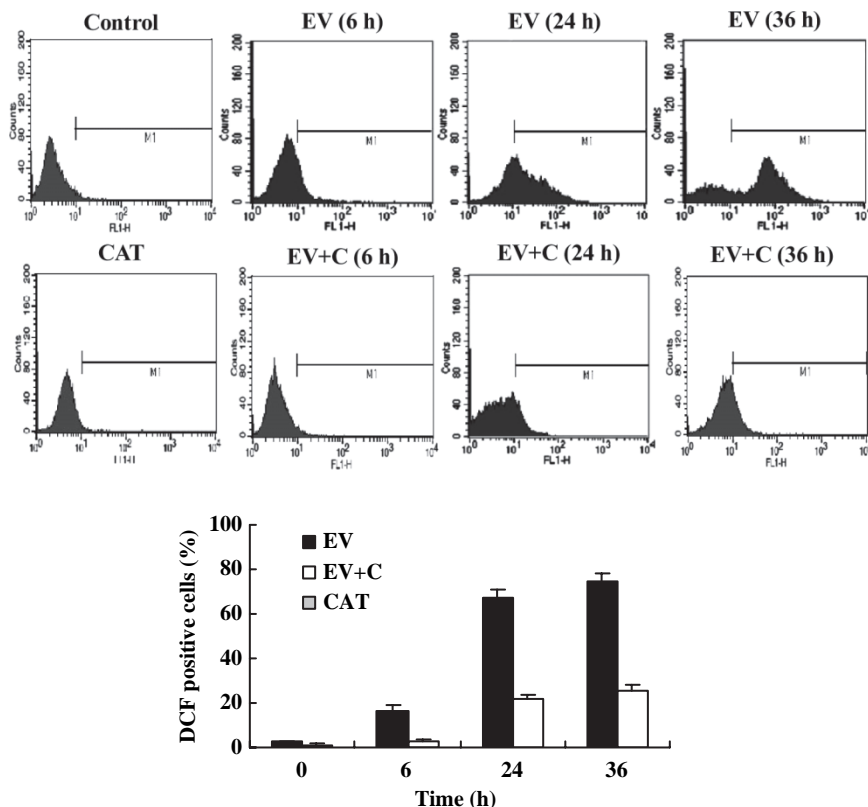


Figure 2. ROS was triggered by evodiamine and could be blocked by CAT. The cells were cultured in the presence of 21 μM evodiamine for 0, 6, 24 or 36 h or coincubated with 1000 U/ml CAT (C) and 21 μM evodiamine for 0, 6, 24 or 36 h. Then the cells were loaded with DCF-DA and examined by flow cytometry. The corresponding linear diagram of the FACScan histograms is expressed at the bottom. Data from a representative experiment ($n=3$) are shown.

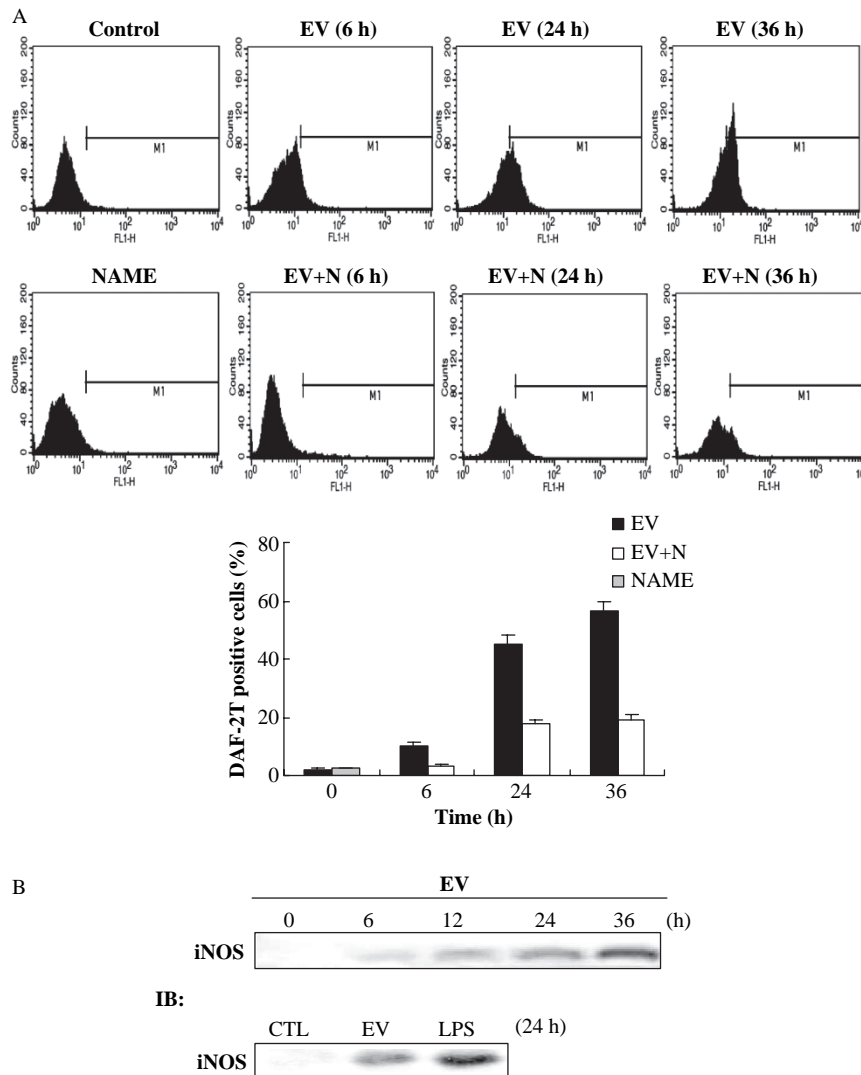


Figure 3. Intracellular NO generation was induced by evodiamine and could be inhibited by L-NAME. (A) The cells were cultured in the presence of 21 μM evodiamine for 0, 6, 24, 36 h or coincubated with 20 mM L-NAME (N) and 21 μM evodiamine for 0, 6, 24, 36 h. DAF-2T, the fluorescent dye product of DAF-2 in reaction with NO, was measured fluorometrically at 1 h post-treatment. The corresponding linear diagram of the FACS histograms was expressed at the bottom. Data from a representative experiment ($n=3$) are shown. (B) The cells were treated with 21 μM evodiamine or 10 $\mu\text{g/ml}$ LPS for the indicated time periods, followed by Western blot analysis for detection of iNOS expression.

dramatic induction of iNOS expression after 12 h. In addition, the protein levels of iNOS expression between evodiamine and endotoxin LPS, a potent inducer of iNOS expression, treated groups were compared at 24 h incubation period; the result showed a strong inductive effect of evodiamine on iNOS expression, with less potent as LPS. Taken together, iNOS expression was induced by evodiamine and contributed to the increased augmentation of NO production in evodiamine-treated HeLa cells.

ROS and NO generation mediated evodiamine-induced apoptosis

To determine the possible lethal roles of ROS and NO induced by evodiamine in HeLa cells, cell viability was measured after drug treatment. Inhibi-

tion of ROS or NO with increasing concentrations of CAT or L-NAME could evidently protect cells from evodiamine-induced cell loss as illustrated by the increased cell viability from 49.34% for evodiamine alone to 62.9% by 500 U/ml CAT, 74.0% by 1000 U/ml CAT, 56.9% by 10 mM L-NAME and 65.5% by 20 mM L-NAME (Figure 4A). Interestingly, when pre-treating HeLa cells with 1000 U/ml CAT and 20 mM L-NAME together, the cell viability was increased to 84.2% (Figure 4A), larger than either CAT or L-NAME alone treatment, indicating that synergistic effects of ROS and NO might be involved. Consistent with the results in Figures 2 and 3, these results confirmed that both ROS and NO production played essential roles in mediating evodiamine-induced HeLa cell death.

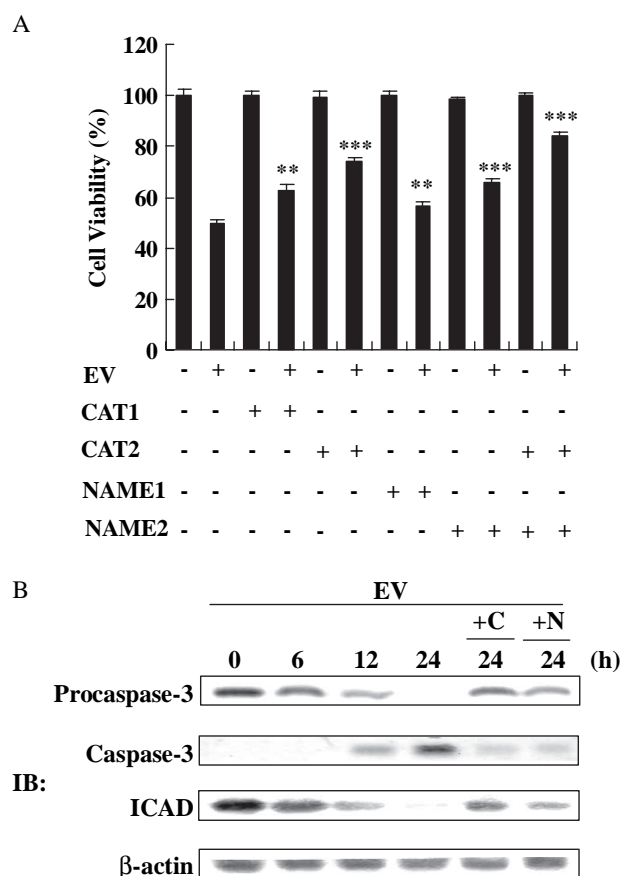


Figure 4. Effects of CAT and L-NAME on evodiamine-induced apoptosis. (A) The cells were cultured in the presence or absence of different doses of CAT or L-NAME for 1 h prior to the addition of 21 μ M evodiamine and then incubated for 24 h. (CAT1: 500 U/ml; CAT2: 1000 U/ml; NAME1: 10 mM; NAME2: 20 mM.) The cell viability was determined by MTT assay ($n=3$). Values are expressed as mean \pm SD. ** $p < 0.01$, *** $p < 0.001$ compared to groups treated with evodiamine alone, as examined by Student's t -test. (B) The cells were treated with 21 μ M evodiamine for the indicated time periods in the presence or absence of 1000 U/ml CAT or 20 mM L-NAME, followed by Western blot analysis for detection of caspase-3 and ICAD expressions.

Since the activation of caspase-3 and the cleavage of DNA fragmentation factor-45 (DFF45)/inhibitor of caspase-3-activated DNase (ICAD) are essential for apoptosis associated with DNA fragmentation [28], to further elucidate the involvement of ROS and NO in apoptosis regulation, we examined both the expressions of caspase-3 and ICAD by Western blot analysis after drug treatment. When caspase-3 is activated by processing, it could cleave DFF45/ICAD. In this study, a time-dependent cleavage of the 32 kD caspase-3 proform into the 17 kD active-form caspase-3 and a significant cleavage of ICAD were both observed after incubation with evodiamine. Pre-incubation with CAT or L-NAME could notably inhibit these processes (Figure 4B). Together, these findings suggested that the apoptosis induced by evodiamine in HeLa cells was regulated by the generated ROS and NO.

Intracellular generated ROS and NO contributed to the dissipation in $\Delta\Psi_m$

To detect whether loss of $\Delta\Psi_m$ was involved in evodiamine-induced HeLa cell apoptosis, the integrity of mitochondrial membranes of HeLa cells was measured by rhodamine 123 staining. Exposure of HeLa cells to evodiamine led to a time-dependent decline in rhodamine positive cells from 95.4% in untreated cells to 72.4% in 6 h- or 50.5% in 24 h-treated cells; pre-incubation with L-NAME or CAT largely enhanced the fluorescent intensity to 63.4% or 73.2%, respectively (Figure 5). Combined pre-treatments with L-NAME and CAT, the rhodamine positive cells were remarkably increased to 88.9% (Figure 5), which was consistent with the result in Figure 4A, indicating that synergistic effects of ROS and NO might be involved. These data demonstrated that notable $\Delta\Psi_m$ dissipation was triggered by evodiamine in HeLa cells, to which ROS and NO contributed greatly.

ROS and NO participated in the Bax translocation, Bcl-2 degradation, Bcl-x_L suppression and cytochrome *c* release

Since $\Delta\Psi_m$ was found to be deprived in the presence of evodiamine, to examine whether the mitochondria-mediated apoptotic pathway participated in evodiamine-induced apoptosis, the expressions of Bax, Bcl-2, Bcl-x_L and cytochrome *c* in cytosolic and mitochondrial fractions were detected by Western blot analysis. Results showed that Bax translocation from cytosol to mitochondria, Bcl-2 degradation, Bcl-x_L suppression and cytochrome *c* release from mitochondria to cytosol were gradually induced by evodiamine treatment and could be reversed by either CAT or L-NAME pre-incubation (Figure 6). Thus, the mitochondria-mediated apoptotic pathway was involved in evodiamine-incubated cells, in which intracellular ROS and NO production played central roles.

ROS and NO were involved in the regulation of autophagy induced by evodiamine

To identify the probable direct induction of HeLa cell autophagy, MDC labelling of autophagosome, the formation of which is the initial step of the autophagic process, was applied. As shown in Figure 7A, the percentage of MDC positive cells in the evodiamine-treated group was 14.7%, 9.2% or 11.0% at 6, 24 or 36 h, respectively, and was significantly higher than that in the control group. However, when 3-MA was introduced, the autophagic percentage was sharply reduced to 2.4–3.3%, almost to the basal level. These data indicate that autophagy was initially triggered by evodiamine at an early stage and decreased later. After pre-treatment with CAT or L-NAME, the

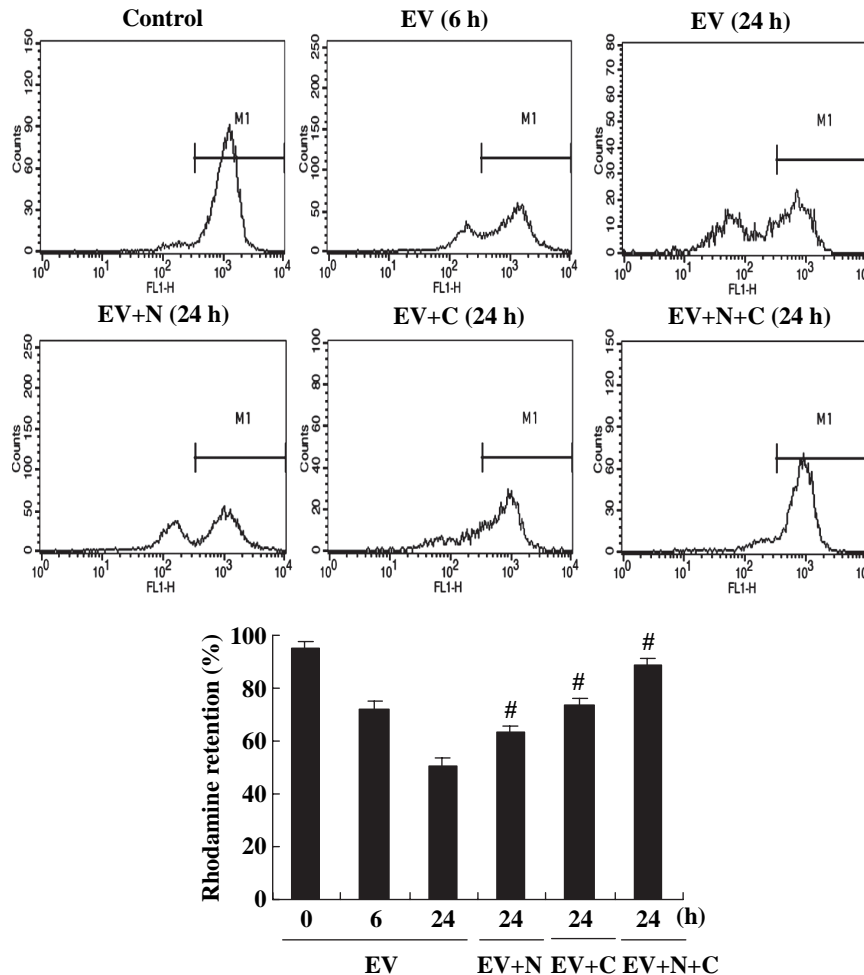


Figure 5. Significant drop in mitochondrial transmembrane potential ($\Delta\Psi_m$) was induced by evodiamine and could be rescued by CAT and L-NAME. The cells were incubated with 21 μM evodiamine for 0, 6, 24 h or coincubated with 1000 U/ml CAT (or/and 20 mM L-NAME) and 21 μM evodiamine for 24 h. Then the cells were loaded with membrane-sensitive probe rhodamine-123 1 $\mu\text{g}/\text{ml}$ at 37°C for 30 min, washed and observed using fluorescence microscopy or measured by FACSscan flow cytometry after collection. The corresponding linear diagram of the FACSscan histograms was expressed at the bottom. Data from a representative experiment ($n=3$) are shown.

proportion of autophagic cells decreased from 14.7% to 5.4% or 7.9% at 6 h, respectively, suggesting the inductive effects of ROS and NO on autophagy. Interestingly, the ratio of autophagic cells was increased from 9.2% to 17.0% or 12.3% in the presence of CAT or L-NAME at 24 h incubation with evodiamine, respectively. Moreover, the autophagic percentage was remarkably increased from 11.0% to 67.4% or 41.2% in the presence of CAT or L-NAME at 36 h incubation with evodiamine, respectively, indicating the inhibitory effects of second stages of ROS and NO on autophagy.

Consistent with the results in Figure 7A, the expression of Beclin 1 in evodiamine-treated cells was observed to be decreased when pre-treated with CAT or L-NAME at 6 h and to be enhanced by pre-incubation with CAT or L-NAME at 36 h (Figure 7B). LC3 has been reported to be cleaved by autophagin (Atg4) to produce the active cytosolic form LC3-I (18 kDa) and then modified in the active form LC3-II (membrane-bounded), which localizes

selectively to forming and newly formed autophagosomes, making LC3-II a useful autophagosomal marker [29]. The LC3 processing in evodiamine-incubated cells was also observed obviously when pre-treated with CAT or L-NAME at 36 h. These significant different effects of CAT or L-NAME on evodiamine-induced autophagy at different time points further suggested that ROS or NO might change their roles in the regulation of autophagy at different culture stages with evodiamine.

Inhibition of autophagy augmented evodiamine-induced cell death

To further determine whether an inductive or preventive effect of autophagy existed in evodiamine-induced cell death, the specific autophagic inhibitor 3-MA was applied. When autophagy was suppressed by 3-MA in evodiamine-treated HeLa cells, the number of apoptotic cells was larger in 3-MA and evodiamine coincubated group and the apoptotic features, including apoptotic bodies, membrane

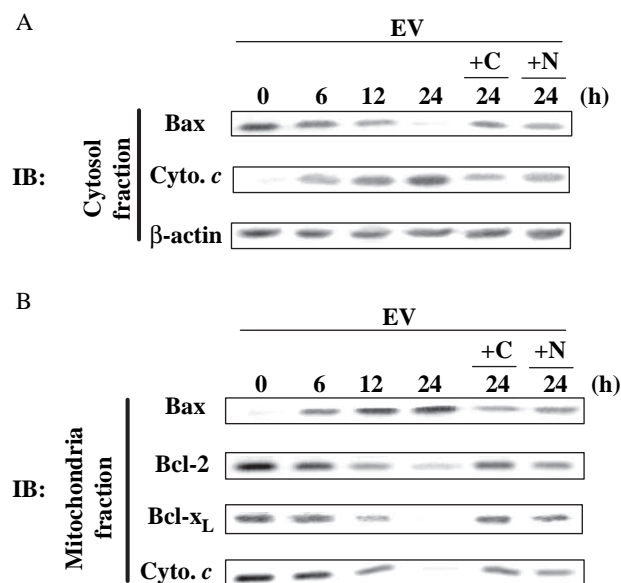


Figure 6. Bax translocation, Bcl-2 degradation, Bcl-x_L suppression and cytochrome *c* release were all induced by evodiamine and could be prevented by CAT and L-NAME. The cells were treated with 21 μM evodiamine for the indicated time periods in the presence or absence of 1000 U/ml CAT or 20 mM L-NAME, followed by Western blot analysis for detection of Bax, Bcl-2, Bcl-x_L and cytochrome *c* expressions both in the cytosol (A) and the mitochondria (B). β-actin was used as an equal loading control.

blebbing, cell becoming round and floating, were more significant (Figure 8A). The cell viability was significantly reduced in a dose-dependent manner at 6, 24 or 36 h, as measured by MTT analysis (Figure 8B). These results suggested that the induced autophagy in evodiamine-treated HeLa cells exerted a protective effect on cell damage for at least 36 h.

Discussion

The role of free radical-mediated reactions in human cancer pathology continues to attract significant interest. In general, it has been shown that different disorders caused by different genetic or environmental insults may have one common molecular basis, namely oxidative stress. Oxidative stress results from exposure to excess levels of free radicals, including ROS and NO, which are not detoxified by cellular antioxidant agents [30]. Evidence has been accumulating that free radical generation can lead to oxidative damage of cell constituents, such as DNA, proteins and lipids. It has been postulated that, depending on the severity of damage, these phenomena result in autophagy, apoptosis or necrosis [31]. Our current experiments further explained the possible roles of ROS and NO in regulating pathways of apoptosis and autophagy.

The results in this study revealed that oxidative stress was induced by evodiamine. The major source of intracellular ROS was possibly H₂O₂ owing to the evident inhibitory effect of CAT, a well-conserved

enzyme which functions to detoxify H₂O₂ and the weakly reducible effect of SOD which functions to detoxify superoxide radicals (data not shown) on ROS production. The enzyme iNOS, which is considered the primary perpetrator of autotoxicity to produce sustained high levels of NO [32], was shown to contribute to the synthesis of NO. Furthermore, a synergistic effect of ROS and NO was found to be involved in evodiamine-induced cell death. This effect is consistent with the reports that NO is essential, together with ROS, for triggering cell death [9]. It was suggested that NO and H₂O₂ could chemically react to produce singlet oxygen or hydroxyl radicals and that these species caused cell death [33]. Superoxide could react with NO to form peroxynitrite, which is extremely reactive and might damage lipid membranes, DNA molecules and proteins, resulting in cell death [34]. Whether the synergistic effect resulted from the interaction between NO and H₂O₂ or superoxide or other mechanisms is currently unknown and needs to be further investigated.

Several enzymes generate ROS including NAD(P)H oxidase, xanthine oxidase, cytochrome P450 and mitochondrial electron transport chain complexes [35]. Mitochondria are the primary site of ROS generation within the cell and are also sensitive targets for ROS because of their phospholipid-containing membranes and the vulnerable mitochondrial DNA [36]. Many studies suggested that ROS participated in the apoptotic process through inducing MMP, which led to the release of cytochrome *c* into the cytosol and thus triggered the apoptotic cascade [37]. The mechanism that can regulate MMP involves the Bcl-2 family of proteins such as Bax, Bcl-2 and Bcl-x_L, which act on the outer mitochondrial membrane to either promote or prevent MMP. In this study, the mitochondrial apoptotic signalling was found to be regulated by ROS/NO via inducing MMP, which might be related to the degradation of Bcl-x_L and Bcl-2, an antioxidant protein considered to detoxify the intracellular ROS [38]. Moreover, a caspase-dependent apoptosis was also found to be regulated by ROS/NO, as demonstrated by the obvious inductive effects of ROS/NO on caspase-3 truncation. This role was probably related to the reported sensitivity of caspase-3 to the alterations of intracellular redox status [39].

Autophagy is a conserved lysosomal degradation pathway that has been extensively studied in recent years [40]. Our study found that autophagy was induced to a maximum level when incubated with evodiamine for a short time and it remained at a low level afterwards. The redox status was proposed to be related to the severity of evodiamine-stimulated autophagy in HeLa cells. It was shown that ROS/NO contributed to the activation of autophagy in a short incubation period and they acted preventively

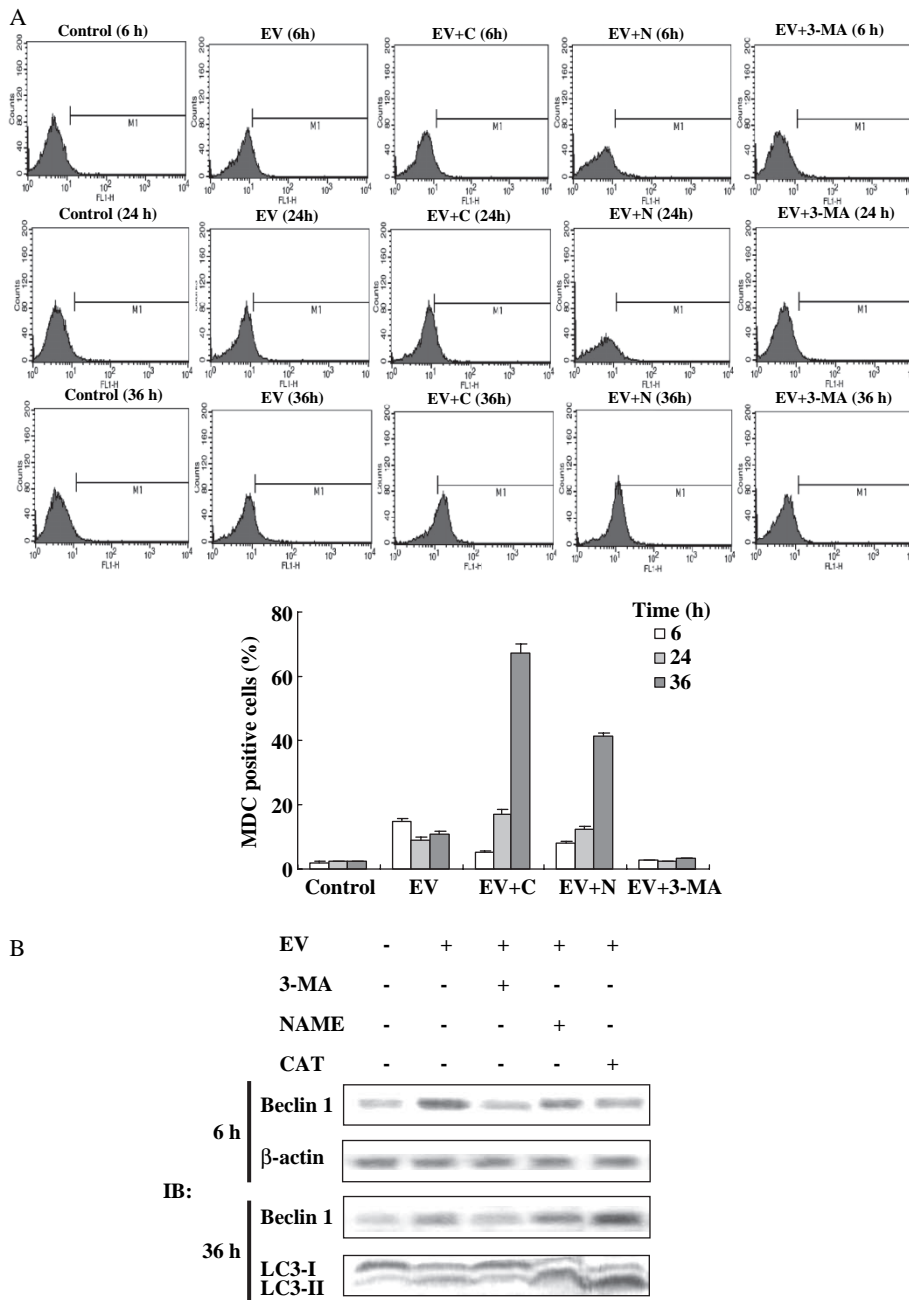


Figure 7. Autophagy was induced by evodiamine and could be affected by pre-treatment with CAT or L-NAME. (A) The cells were incubated with 21 μ M evodiamine for 6, 24 or 36 h in the absence or presence of 1000 U/ml CAT, 20 mM L-NAME or 4 mM 3-MA. Then the cells were labelled with MDC and the autophagic ratio was measured by flow cytometry. The corresponding linear diagram of the FACSscan histograms is expressed at the bottom. Data from a representative experiment ($n = 3$) are shown. (B) The cells were treated with 21 μ M evodiamine for 6 or 36 h in the presence or absence of 1000 U/ml CAT, 20 mM L-NAME or 4 mM 3-MA, followed by Western blot analysis for detection of Beclin 1 or LC3. β -actin was used as an equal loading control.

to autophagy through a long incubation period. Such reports have demonstrated that ROS can exert an inductive effect on autophagy, the mechanism of which has been suggested to be related to its specific regulation of the activity of Atg4 [41]. On the other hand, free radicals may inhibit autophagy by directly damaging the lysosomal membrane to an extent that results in the leakage of lysosomal hydrolases out to the cytosol during massive acute oxidative stress [42]. In this study, it was found that ROS/NO could

diversely regulate autophagy through modulating Beclin 1, a Bcl-2 interacting protein, which controls autophagy in a class III phosphoinositide 3-kinase (PI3K)-dependent manner as reported [43], in response to their severity. The massive ROS/NO could also prevent autophagy through inhibiting the processing of LC3 to a membrane-bound form LC3-II, which becomes membrane-associated and preferentially associating with the developing and newly formed autophagosomes. Consistent with the reports,

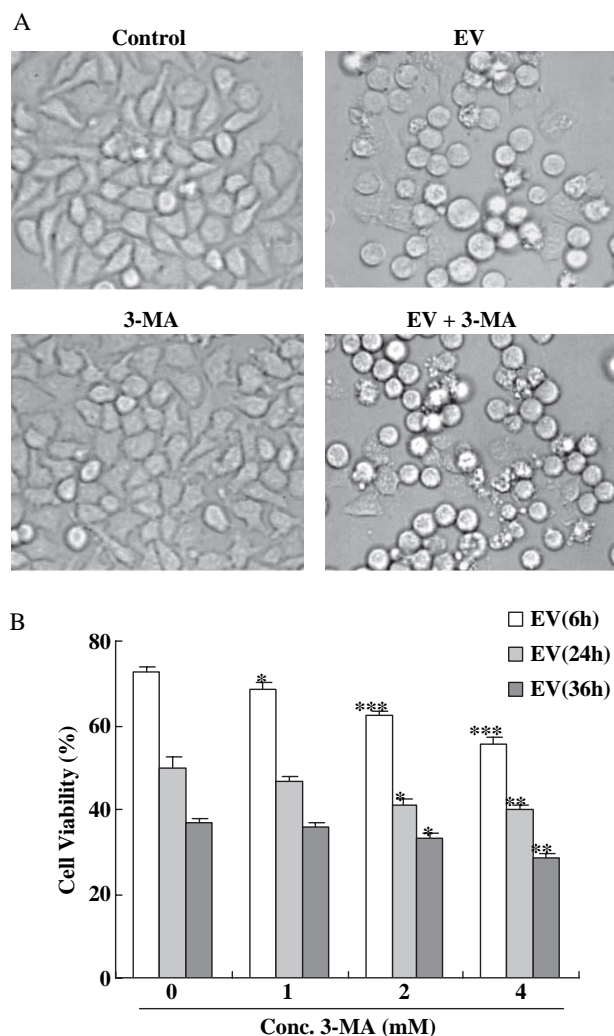


Figure 8. 3-MA exerted an enhance effect on evodiamine-induced cell death. (A) The cellular morphologic changes were observed after cells incubated with medium, 4 mM 3-MA, 21 μ M evodiamine or 4 mM 3-MA plus 21 μ M evodiamine for 24 h under a phase contrast microscope ($\times 200$ magnification). (B) The cells were treated with 21 μ M evodiamine for 6, 24 or 36 h in the presence or absence of 1, 2 or 4 mM 3-MA, followed by MTT analysis ($n=3$). * $p < 0.05$, ** $p < 0.01$, *** $p < 0.001$ compared to groups treated with evodiamine alone at the corresponding time points, as examined by Student's t -test.

our findings reflected that the autophagic process could be regulated differently in response to the alteration of intracellular redox status.

The interplay between autophagy and apoptosis is complex, with the accumulating data revealing cases in which autophagy is an antagonistic, agonistic or independent of canonical programmed cell death via the apoptotic pathway [44]. By observation of the inductive effect of 3-MA on evodiamine-induced ROS/NO-dependent cell loss, autophagy was found primarily to be a survival strategy in evodiamine-treated HeLa cells. Upregulation of this system has been reported to play a significant role in adaptation

to environments where oxidative stress is a major selection pressure and where the process can rapidly delete and recycle oxidatively damaged proteins and organelles [45]. And it has been shown that 3-MA has a potent inhibitory effect on PI3K activity *in vitro* studies. The enzyme class III PI3K, which synthesizes the phosphatidylinositol 3-phosphate (PtdIns3P) from PtdIns, is essential for the formation of the autophagosome. The preventive effect of 3-MA on intracellular trafficking of proteins from late endosomes to lysosomes is also suggested to be compatible with the requirement of PI3K at this step [46]. Thus, class III PI3K might function in the promotive effect of autophagy on cell viability as elicited by the results from 3-MA administration. Together with the above findings, it was revealed that autophagy acted to provide defense against cell death in response to mild oxidative stress; whereas it was inhibited by severe oxidative stress, where the apoptosis prevailed. This study provides evidence that autophagy serves as an adaptive mechanism facilitating cancer cell survival and resistance to therapy-induced apoptosis and the inhibitor of autophagy can enhance the efficacy of therapeutic strategies designed to induce cancer cell apoptosis.

In summary, the present results indicated that the productions of ROS and NO were both triggered by evodiamine and they acted in synergy to promote a mitochondria- and caspase-dependent apoptosis. Importantly, autophagy was found to be stimulated by evodiamine and regulated complexly by ROS/NO. Moderate ROS/NO contributed to the activation of autophagy in order to protect cells against damage under a mild oxidative stress; whereas massive ROS/NO played negative roles in the autophagic process under a severe oxidative stress, where the irreversibly damaged cells were removed by apoptosis.

Declaration of interest: The authors report no conflicts of interest. The authors alone are responsible for the content and writing of the paper.

References

- [1] Ameisen JC. On the origin, evolution, and nature of programmed cell death: a timeline of four billion years. *Cell Death Differ* 2002;9:367–393.
- [2] Fadeel B, Orrenius S, Zhivotovsky B. Apoptosis in human disease: a new skin for the old ceremony? *Biochem Biophys Res Commun* 1999;266:699–717.
- [3] Birbes H, El Bawab S, Hannun YA, Obeid LM. Selective hydrolysis of a mitochondrial pool of sphingomyelin induces apoptosis. *FASEB J* 2001;15:2669–2679.
- [4] Jacotot E, Ferri KF, El Hamel C, Brenner C, Druillennec S, Hoebeke J, Rustin P, Métévier D, Lenoir C, Geuskens M, Vieira HL, Loeffler M, Belzacq AS, Briand JP, Zamzami N,

- Edelman L, Xie ZH, Reed JC, Roques BP, Kroemer G. Control of mitochondrial membrane permeabilization by adenine nucleotide translocator interacting with HIV-1 viral protein rR and Bcl-2. *J Exp Med* 2001;193:509–519.
- [5] Deretic V. Autophagy in innate and adaptive immunity. *Trends Immunol* 2005;26:523–528.
- [6] Amaravadi RK, Yu D, Lum JJ, Bui T, Christophorou MA, Evan GI, Thomas-Tikhonenko A, Thompson CB. Autophagy inhibition enhances therapy-induced apoptosis in a Myc-induced model of lymphoma. *J Clin Invest* 2007;117:326–336.
- [7] Gutierrez MG, Master SS, Singh SB, Taylor GA, Colombo MI, Deretic V. Autophagy is a defense mechanism inhibiting BCG and Mycobacterium tuberculosis survival in infected macrophages. *Cell* 2004;119:753–766.
- [8] Dröge W. Free radicals in the physiological control of cell function. *Physiol Rev* 2002;82:47–95.
- [9] Zaninotto F, La Camera S, Polverari A, Delledonne M. Cross talk between reactive nitrogen and oxygen species during the hypersensitive disease resistance response. *Plant Physiol* 2006;141:379–383.
- [10] Zhang Y, Wu LJ, Tashiro S, Onodera S, Ikejima T. Evodiamine induces tumor cell death through different pathways: apoptosis and necrosis. *Acta Pharmacol Sin* 2004;25:83–89.
- [11] Kobayashi Y, Nakano Y, Kizaki M, Hoshikuma K, Yokoo Y, Kamiya T. Capsaicin-like anti-obese activities of evodiamine from fruits of *Evodia rutaecarpa*, a vanilloid receptor agonist. *Planta Med* 2001;67:628–633.
- [12] Yamahara J, Yamada T, Kitani T, Naitoh Y, Fujimura H. Antianoxic action of evodiamine, an alkaloid in *Evodia rutaecarpa* fruit. *J Ethnopharmacol* 1989;27:185–192.
- [13] Kobayashi Y. The nociceptive and anti-nociceptive effects of evodiamine from fruits of *Evodia rutaecarpa* in mice. *Planta Med* 2003;69:425–428.
- [14] Chiou WF, Chou CJ, Shum AY, Chen CF. The vasorelaxant effect of evodiamine in rat isolated mesenteric arteries: mode of action. *Eur J Pharmacol* 1992;215:277–283.
- [15] Yang J, Wu LJ, Tashiro S, Onodera S, Ikejima T. Critical roles of reactive oxygen species in mitochondrial permeability transition in mediating evodiamine-induced human melanoma A375-S2 cell apoptosis. *Free Radic Res* 2007;41:1099–1108.
- [16] Yang J, Wu LJ, Tashiro S, Onodera S, Ikejima T. Nitric oxide activated by p38 and NF-kappaB facilitates apoptosis and cell cycle arrest under oxidative stress in evodiamine-treated human melanoma A375-S2 cells. *Free Radic Res* 2008;42:1–11.
- [17] Jarrett SG, Albon J, Boulton M. The contribution of DNA repair and antioxidants in determining cell type-specific resistance to oxidative stress. *Free Radic Res* 2006;40:1155–1165.
- [18] Charrier L, Jarry A, Toquet C, Bou-Hanna C, Chedorge M, Denis M, Vallette G, Laboisse CL. Growth phase-dependent expression of ICAD-L/DFF45 modulates the pattern of apoptosis in human colonic cancer cells. *Cancer Res* 2002;62:2169–2174.
- [19] Vaidyanathan R, Scott TW. Apoptosis in mosquito midgut epithelia associated with West Nile virus infection. *Apoptosis* 2006;11:1643–1651.
- [20] Yang ML, Huang TS, Lee Y, Lu FJ. Free radical scavenging properties of sulfapyrazone. *Free Radic Res* 2002;36:685–693.
- [21] Habel ME, Jung D. Free radicals act as effectors in the growth inhibition and apoptosis of iron-treated Burkitt's lymphoma cells. *Free Radic Res* 2006;40:789–797.
- [22] Venkataraman S, Wagner BA, Jiang X, Wang HP, Schafer FQ, Ritchie JM, Patrick BC, Oberley LW, Buettner GR. Overexpression of manganese superoxide dismutase promotes the survival of prostate cancer cells exposed to hyperthermia. *Free Radic Res* 2004;38:1119–1132.
- [23] Zhou B, Wu LJ, Li LH, Tashiro S, Onodera S, Uchiyama F, Ikejima T. Silibinin protects against isoproterenol-induced rat cardiac myocyte injury through mitochondrial pathway after up-regulation of SIRT1. *J Pharmacol Sci* 2006;102:387–395.
- [24] Zanna C, Ghelli A, Porcelli AM, Martinuzzi A, Carelli V, Rugolo M. Caspase-independent death of Leber's hereditary optic neuropathy cybrids is driven by energetic failure and mediated by AIF and Endonuclease G. *Apoptosis* 2005;10:997–1007.
- [25] Fu L, Pelicano H, Liu J, Huang P, Lee C. The circadian gene Period2 plays an important role in tumor suppression and DNA damage response *in vivo*. *Cell* 2002;111:41–50.
- [26] Biederbeck A, Kern HF, Elsässer HP. Monodansylcadaverine (MDC) is a specific *in vivo* marker for autophagic vacuoles. *Eur J Cell Biol* 1995;66:3–14.
- [27] Takahama U, Hirota S, Oniki T. Production of nitric oxide-derived reactive nitrogen species in human oral cavity and their scavenging by salivary redox components. *Free Radic Res* 2005;39:737–745.
- [28] Jänicke RU, Sprengart ML, Wati MR, Porter AG. Caspase-3 is required for DNA fragmentation and morphological changes associated with apoptosis. *J Biol Chem* 1998;273:9357–9360.
- [29] Ferraro E, Cecconi F. Autophagic and apoptotic response to stress signals in mammalian cells. *Arch Biochem Biophys* 2007;462:210–219.
- [30] Aksenova MV, Aksenov MY, Mactutus CF, Booze RM. Cell culture models of oxidative stress and injury in the central nervous system. *Curr Neurovasc Res* 2005;2:73–89.
- [31] Lemasters JJ, Nieminen AL, Qian T, Trost LC, Elmore SP, Nishimura Y, Crowe RA, Cascio WE, Bradham CA, Brenner DA, Herman B. The mitochondrial permeability transition in cell death: a common mechanism in necrosis, apoptosis and autophagy. *Biochim Biophys Acta* 1998;1366:177–196.
- [32] Bogdan C. The multiplex function of nitric oxide in (auto)immunity. *J Exp Med* 1998;187:1361–1365.
- [33] Noronha-Dutra AA, Epperlein MM, Woolf N. Reaction of nitric oxide with hydrogen peroxide to produce potentially cytotoxic singlet oxygen as a model for nitric oxide-mediated killing. *FEBS Lett* 1993;321:59–62.
- [34] Fenster CP, Weinsier RL, Darley-Usmar VM, Patel RP. Obesity, aerobic exercise, and vascular disease: the role of oxidant stress. *Obes Res* 2002;10:964–968.
- [35] Wolin MS. Interactions of oxidants with vascular signaling systems. *Arterioscler Thromb Vasc Biol* 2000;20:1430–1442.
- [36] Wei YH, Lee HC. Oxidative stress, mitochondrial DNA mutation, and impairment of antioxidant enzymes in aging. *Exp Biol Med (Maywood)* 2002;227:671–682.
- [37] Li D, Das S, Yamada T, Samuels HH. The NRIF3 family of transcriptional coregulators induces rapid and profound apoptosis in breast cancer cells. *Mol Cell Biol* 2004;24:3838–3848.
- [38] Giardino I, Edelstein D, Brownlee M. BCL-2 expression or antioxidants prevent hyperglycemia-induced formation of intracellular advanced glycation endproducts in bovine endothelial cells. *J Clin Invest* 1996;97:1422–1428.
- [39] Rosati E, Sabatini R, Ayroldi E, Tabilio A, Bartoli A, Bruscoli S, Simoncelli C, Rossi R, Marconi P. Apoptosis of human primary B lymphocytes is inhibited by N-acetyl-L-cysteine. *J Leukoc Biol* 2004;76:152–161.
- [40] Chen Y, Gibson SB. Is mitochondrial generation of reactive oxygen species a trigger for autophagy? *Autophagy* 2008;4:246–248.
- [41] Kiffin R, Bandyopadhyay U, Cuervo AM. Oxidative stress and autophagy. *Antioxid Redox Signal* 2006;8:152–162.

- [42] Kaushik S, Cuervo AM. Autophagy as a cell-repair mechanism: activation of chaperone-mediated autophagy during oxidative stress. *Mol Aspects Med* 2006;27:444–454.
- [43] Kihara A, Kabeya Y, Ohsumi Y, Yoshimori T. Beclin-phosphatidylinositol 3-kinase complex functions at the trans-Golgi network. *EMBO Rep* 2001;2:330–335.
- [44] Lockshin RA, Zakeri Z. Apoptosis, autophagy, and more. *Int J Biochem Cell Biol* 2004;36:2405–2419.
- [45] Moore MN, Allen JI, Somerfield PJ. Autophagy: role in surviving environmental stress. *Mar Environ Res* 2006;62: S420–S425.
- [46] Cui Q, Tashiro S, Onodera S, Minami M, Ikejima T. Autophagy preceded apoptosis in oridonin-treated human breast cancer MCF-7 cells. *Biol Pharm Bull* 2007;30:859–864.